



Artocarpus odoratissimus skin as a potential low-cost biosorbent for the removal of methylene blue and methyl violet 2B

Linda B.L. Lim^{a,*}, Namal Priyantha^{b,c}, Chieng Hei Ing^a, Muhd Khairud Dahri^a, D.T.B. Tennakoon^a, Tasneem Zehra^a, Montri Suklueng^d

^aFaculty of Science, Department of Chemistry, Universiti Brunei Darussalam, Jalan Tungku Link, Gadong, Brunei Darussalam
Tel. 00 673 8748010; Fax: 00 673 2461502; email: linda.lim@ubd.edu.bn

^bFaculty of Science, Department of Chemistry, University of Peradeniya, Peradeniya, Sri Lanka

^cPostgraduate Institute of Science, University of Peradeniya, Peradeniya, Sri Lanka

^dEnergy Research Group, Universiti Brunei Darussalam, Jalan Tungku Link, Gadong, Brunei Darussalam

Received 3 June 2013; Accepted 17 September 2013

ABSTRACT

Artocarpus odoratissimus (Tarap) skin shows great potential as an effective low-cost biosorbent for toxic dyes, methylene blue (MB), and methyl violet 2B (MV). The Langmuir adsorption isotherm leads to the maximum biosorption capacities of this biomass, whose point of zero charge was at pH 4.4, of 0.577 mmol g⁻¹ (184.6 mg g⁻¹) and 0.349 mmol g⁻¹ (137.3 mg g⁻¹) for MB and MV, respectively. The Sips isotherm model is the best fit for adsorption of MB, while both the Langmuir and Sips models are in good agreement for MV. Mass transfer of dye species from solution to the biosorbent phase is fast with 50% dye being removed in less than 1 min following the pseudo-second-order kinetics.

Keywords: *Artocarpus odoratissimus*; Biosorption; Methylene blue; Methyl violet 2B; Kinetics

1. Introduction

With the rapid population growth over the past few decades, industrialization has expanded significantly to cater for the huge demand of humans. This in turn has resulted in an increase in the amount of pollutants being released into the environment, especially to water resources. Consequently, there is an urgent need to find means of reducing water pollution as it poses many health and environmental effects. Although various methods, including ion-exchange, chemical precipitation, ultrafiltration, photocatalytic oxidation, and ozonation, have been reported [1–4], some of these methods are neither effective nor economical. In the last two decades, attention has been

shifted towards searching for low-cost biosorbents for the removal of environmental pollutants, as an effective remedial measure [5].

The use of industrial/food waste to clean up the environment has become attractive, as such waste is not only unused resources but also associated with disposal problems [6,7]. Biosorption therefore provides a two-fold advantage in solving environmental pollution problems. The use of waste materials would lead to the reduction of the amount of waste being discarded and low-cost treatment of wastewater. To date, many different types of natural substances and waste materials, including agricultural waste, industrial byproducts and wastes, peat, and clay have been used to remove pollutants [7–13]. Due to the vast biosorbents available, the challenge is to find highly

*Corresponding author.

promising biosorbents that can effectively bind with the selected environmental pollutants.

Artocarpus odoratissimus (*Artocarpus tarap* Becc. or *Artocarpus mutabilis* Becc.) is a popular seasonal fruit widely cultivated in Brunei Darussalam. Its English name is “Marang” while the local name is “Tarap,” and its maximum diversity occurs in Brunei Darussalam. The fruit of *A. odoratissimus* consists of skin, core, flesh, and seed. Inside the fruit is the edible flesh which clings to a central core and each segment of this flesh has a seed inside it. The inedible part of the fruit (skin and core) is found to comprise of >60% of the total mass [14], which is discarded without being utilized. Our recent findings have shown that the core and/or skin of both *A. odoratissimus* and *A. altilis* were able to remove Cu(II) and Cd(II) ions within a short period of contact time [15,16]. As an extension to this finding, we explore the possibility of the potential utilization of the *A. odoratissimus* skin as means to remove toxic dyes from aqueous solutions. To the best of our knowledge, there have been no reported studies on the use of *A. odoratissimus* waste for the removal of toxic dyes.

2. Materials and methods

2.1. Chemicals and reagents

A 1,000 mg L⁻¹ stock solution of each dye, methylene blue (MB) or methyl violet 2B (MV) (Sigma-Adrich), was prepared by dissolving the dye in distilled water, which was subsequently diluted to prepare a series of dye concentrations ranging from 10 to 1,000 mg L⁻¹. Solutions of different pH were prepared using 0.1 M NaOH and 0.1 M HNO₃, both of which were purchased from Fluka. All chemicals were used without further purification.

2.2. Sample preparation and general aspects

Randomly selected fruit samples were bought from the local open markets in the Brunei-Muara District of Brunei Darussalam. The skin was separated from the rest of the fruit and oven dried at 80°C until a constant mass was obtained. The dried sample was then blended and sieved to obtain the fraction of the particle sizes between 355 and 850 μm. The sieved sample was thoroughly mixed prior to using them for experiments in order to ensure the uniformity. All experiments were done in duplicate/triplicate.

2.3. Characterization of Tarap skin

The point of zero charge (pH_{pzc}) was determined using the solid addition method [17,18] as described

below. The pH_{pzc} of Tarap skin was determined by using 0.1 M KNO₃ solution and adjusted to the required pH (2, 4, 6, 10, and 12) by the addition of 0.1 M HNO₃ and 0.1 M NaOH. Each KNO₃ solution (25.0 mL) maintained at a particular pH was added into each of the flask containing pre-weighed Tarap skin (0.050 g), and agitated on an orbital shaker at 250 rpm for 24 h. The graph of ΔpH (difference between the initial and the final pHs of KNO₃ solution) against pH_i (initial pH) was then plotted to determine the point of zero charge of Tarap skin.

2.4. Instrumentation

UV–Vis spectrophotometer (Shimadzu/Model UV-1601PC) was used for measurement of absorbance of dye solutions at λ_{max} of 664.4 nm (MB) and 584.0 nm (MV), while FTIR spectrophotometer (Shimadzu Model IRPrestige-21) was used for measurements of solids. C, H, N, and S contents present in Tarap skin were determined in the Elemental Analysis Laboratory at the National University of Singapore, while X-ray fluorescence (XRF) spectrophotometer (PANalytical Axios^{max}) was used to determine the other elements. Tescan Vega XMU scanning electron microscope (SEM) was used to investigate the morphological characteristics of the adsorbent surface and the coating of the biosorbent was done using SPI-MODULETM Sputter Coater.

2.5. Optimization of parameters

All optimization experiments were performed by mixing the biosorbent and 10.0 mg L⁻¹ dye solution in a ratio of 1:500 at ambient temperature, followed by shaking at a constant speed of 250 rpm. The extent of dye removed in each solution was then determined through absorbance measurements of filtrates, obtained using a fine metal sieve, at the respective λ_{max} value.

The effect of shaking time was investigated using different shaking time periods from 30 to 240 min, and the effect of settling time was determined by shaking the samples for the optimum shaking time, followed by allowing to settle for different time periods up to 240 min. The effect of medium pH was carried out by determining the extent of removal of each dye solution of different pH in the range from 2.0 to 9.0, after allowing for optimized shaking and settling time periods.

Pre-treatment of the biosorbent by acidification, basification, and washing was carried out by shaking the sample in 1 M HNO₃, 1 M NaOH, and distilled

water, respectively, for 2 h. Samples were thoroughly washed with distilled after acidification and basification. All pre-treated samples were dried prior to being used.

2.6. Isotherm analysis

Each biosorbent sample was treated with a dye solution of a concentration varying from 0 mg L⁻¹ to 1,000 mg in 1:500 solid/solution ratio, and shaken at 250 rpm for the optimum shaking and settling times, and allowed to settle for the optimum time period. The solution was filtered using fine metal sieve, and the absorbance of the filtrate was determined.

2.7. Kinetics studies of biosorption

Each biosorbent (0.10 g) was mixed with 10.0 mg L⁻¹ of each dye solution (50.0 mL) separately, and the suspensions were stirred at 250 rpm at ambient temperature immediately after mixing. Samples were then withdrawn from each solution after different reaction time periods with one minute apart until the equilibrium was reached. Each solution was filtered using fine metal sieve, and the filtrate was analyzed.

3. Results and discussion

3.1. Characterization of Tarap skin

Elemental analysis of Tarap skin shows that it contains 42.34% C, 5.32% H, 0.98% N, and 0.50% S. Characterization of elements by XRF shows that potassium was present in the highest amount followed by zinc and iron (Table 1). It can be seen from Fig. 1 that adsorption with dyes reduced the amounts of potassium and iron present. This effect is greater for MB than MV, where in the case of potassium, it was reduced from 39.8 to 6.6% and 12.3% for MB and MV, respectively. For iron, the amount was reduced from 5.2 to 1.9% for MB and 2.3% for MV. As the dyes investigated are cationic in nature, there is a possibility to replace metals, such as K and Fe, which could be present in their cationic form at a high concentration without having strong binding.

3.1.1. SEM of Tarap skin before and after treatment with dyes

The surface morphology of Tarap skin before and after sorption of 1,000 mg L⁻¹ dye solutions is shown in Fig. 2. It can be seen from Fig. 2(i) that the surface of Tarap skin is very rough and uneven in nature with

Table 1
Characterization of elements present in Tarap skin by XRF

Element	Normalized percentage (%)
O	24.1
Mg	1.4
Al	0.2
Si	1.6
P	1.6
S	1.8
Cl	2.8
K	39.8
Ca	4.9
Mn	0.5
Fe	5.2
Zn	14.0
Rb	0.2
Zr	0.10
Ru	2.0

pores and cavities which are able to provide large surface area for the sorption of dyes. The surface morphology has significantly changed on treatment with dye confirming the sorption of dye molecules (Fig. 2(ii) and 2(iii)).

3.1.2. Effect of contact time

Prior to sorption equilibrium studies, it is important to establish the time required for each of the dyes to reach equilibrium upon contact with Tarap skin. This is especially significant in treatment of wastewater by means of adsorption techniques, whereby a rapid uptake of adsorbate by an adsorbent signifies the efficacy of the adsorbent to be used in wastewater treatment. Under the experimental conditions employed in this study, it can be seen from Fig. 3 that both MB and MV exhibit a similar trend and that the percentage removal curve is indicative of a possible monolayer adsorption. The adsorption of both dyes was rapid within the initial 30 min period showing more than 60% removal. Thereafter, it gradually slows down and reaches equilibrium at about 3.5 h, and hence the optimum shaking time was taken as 4.0 h.

It can be seen that the contact time for adsorption of MB on Tarap skin is comparable with that on coconut waste [19] and jackfruit [20], which is another *Artocarpus* species, and shorter when compared to other low-cost biosorbents, such as pomelo peel [21] and tea waste [22].

With the optimized shaking time of 4.0 h, the system should be allowed to rest since, unlike in homogenous systems, the adsorbates in liquid/solid heterogeneous systems usually undergo various mass transfer steps, some of which could be relatively

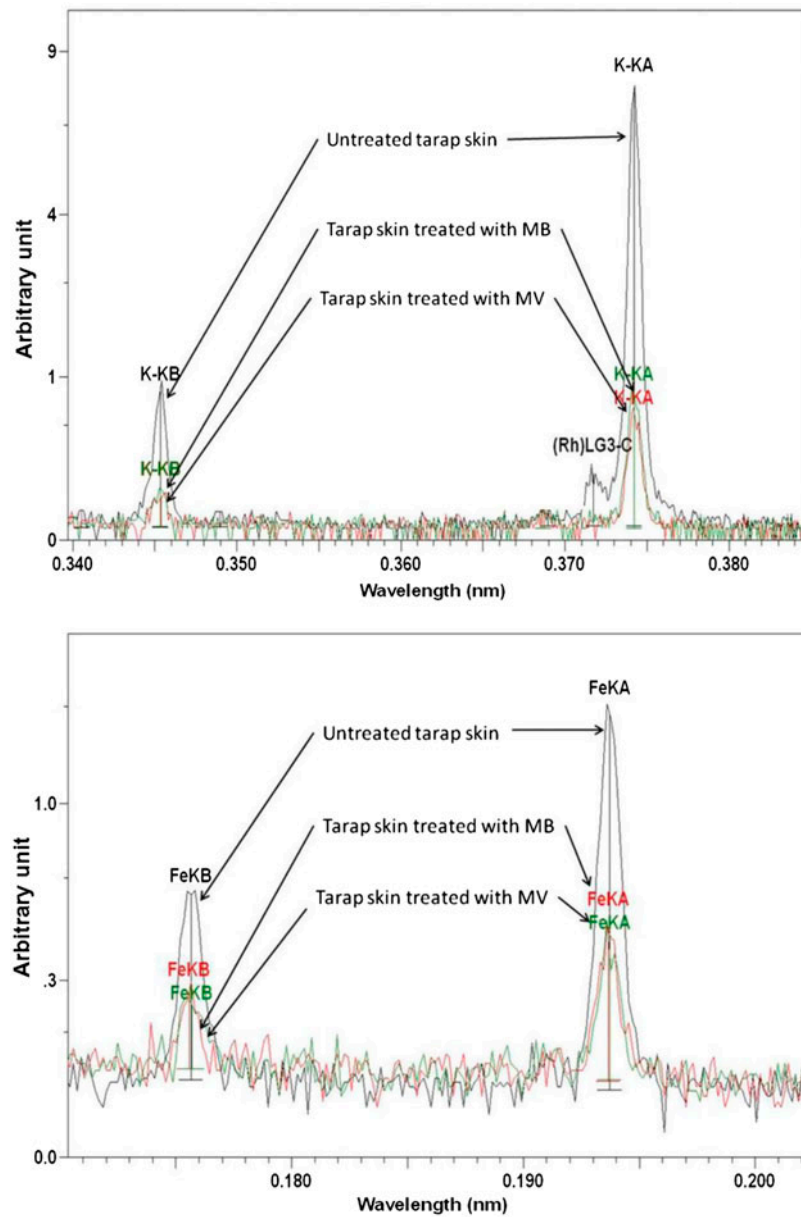


Fig. 1. XRF of Tarap skin showing potassium (top) and iron (bottom) before and after adsorption with $1,000 \text{ mg L}^{-1}$ MB and MV.

slow. Hence, it is important to optimize settling time to ensure that the equilibrium is reached. It was experimentally observed that the percentage removal of each dye, after allowing the optimized shaking time, does not change with settling time after 30 min. Consequently, 1.0 h settling time was selected as the optimum.

3.2. Effect of medium pH

Medium pH plays a significant role in the uptake of adsorbates by biosorbents as the pH would cause

the surface charge to alter, thereby affecting the efficiency of biosorbents.

The point of zero charge (pH_{pzc}), which is the point at which the ΔpH vs pH_i curve intersects the pH axis, is found to be at approximately pH 4.4 (Fig. 4), indicating that the surface charge is zero at this pH. Hence, the surface of the adsorbent is positively charged at pH lower than pH_{pzc} and negatively charged if the pH is greater than the pH_{pzc} . The pH_{pzc} of jackfruit skin is reported to be 3.9 [20], which is comparable to that of Tarap skin.

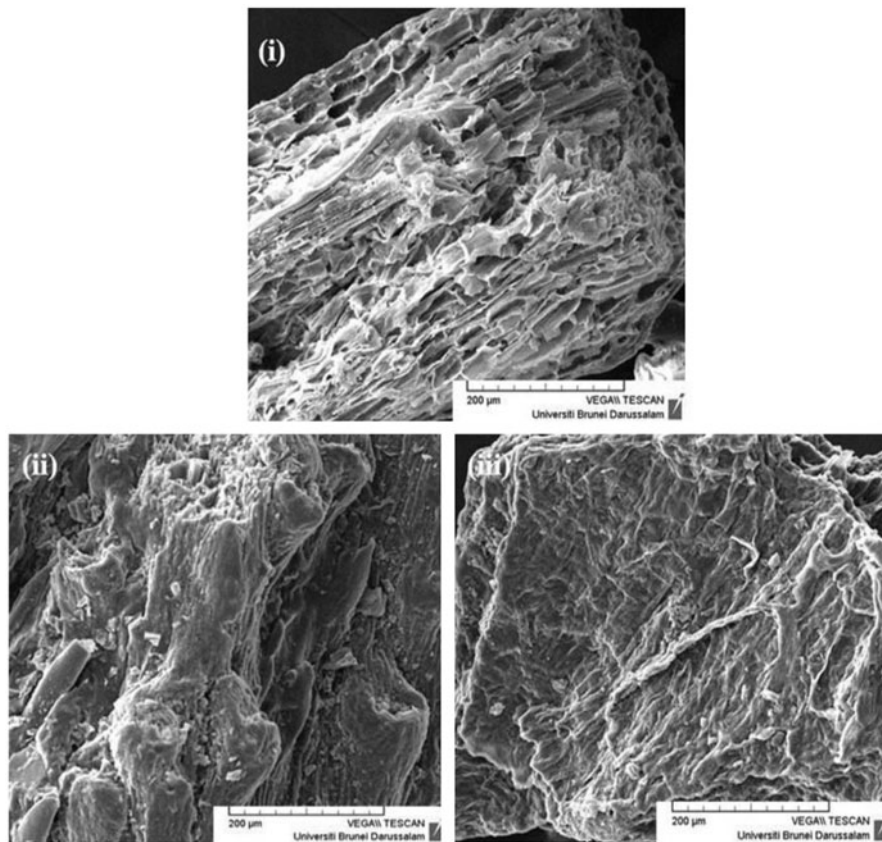


Fig. 2. Tarap skin at 500x magnification (i) before sorption of dye, (ii) after sorption with MB, and (iii) after sorption with MV.

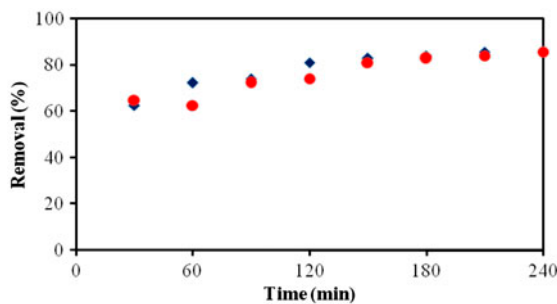


Fig. 3. Effect of shaking time on the extent of removal of each dye by Tarap skin; MB (◆) and MV (●).

Fig. 5 shows that there is a decrease in the extent of adsorption of both MB and MV on Tarap skin at pH 2. This effect is greater for MB with a drastic decrease of 66% as opposed to 9% for MV. This decrease can be explained due to the positive surface charge of Tarap skin as a result of protonation at pH = 2 which is less than pH_{pZC} resulting in electrostatic repulsion. Similar effect has been reported for

other low-cost biosorbents, such as jackfruit leaf [23]. Being both cationic dyes, the greater extent of adsorption of MB as compared to that of MV is probably due to the difference in the molecular size and the chemical nature. Since the amount of dye being removed was high (>80%) at ambient pH (MB = 4.6, MV = 5.99), as compared to that at other pHs, all subsequent experiments throughout this study were carried out without any alteration to the ambient pH.

3.3. Effect of pretreatment of biosorbent

Investigation of the effect of pretreatment of Tarap skin by both acids and bases as well as by washing the biosorbent in distilled water did not show much improvement in the biosorption ability towards MB (Fig. 6). However, an increase of 9% was observed for the adsorption of MV when the Tarap skin was washed with distilled water, and its pretreatment with acid/base enhanced by 17%. Consequently, washed Tarap skin was used for all subsequent experiments with both MB and MV.

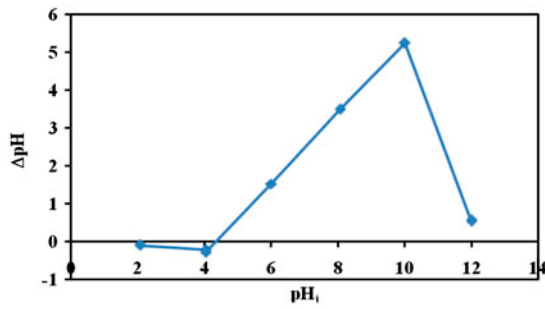


Fig. 4. Variation of ΔpH with the initial solution pH at a shaking time period of 24.0 h and setting time period of 1.0 h.

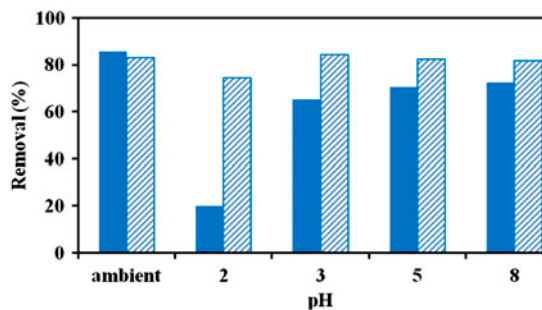


Fig. 5. Effect of medium pH on biosorption of Tarap skin for MB (■) and MV (▨).

3.4. Adsorption isotherms

In order to understand the interaction of dyes with Tarap skin, adsorption studies were carried out under optimized contact time with dye concentrations ranging from 10.0 to 1,000 mg L^{-1} . According to Fig. 7, the extent of adsorption of both MB and MV on Tarap skin follow the L-type adsorption according to Giles's classification [24]. Such L-curve indicates that, as the adsorption sites are being filled, there is progressively less chance of the adsorbate molecules finding suitable sites to be adsorbed. L-curve also suggests that either

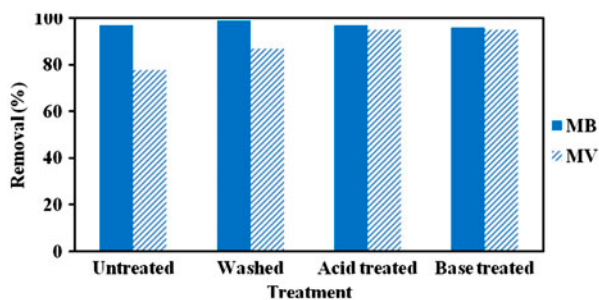


Fig. 6. Extent of dye removal by Tarap skin treated with water, acid and base for MB (■) and MV (▨).

the adsorbate lies with the flat orientation on the surface or there is a lack of strong competition between solvent and the adsorbate for the surface sites of the adsorbent.

The equilibrium data obtained from adsorption studies of the two dyes were used to model six different isotherm models, namely the Langmuir [25], Freundlich [26], Temkin [27], Dubinin–Radushkevich (D–R) [28], Redlich–Peterson (R–P) [29], and Sips [30] (Tables 2 and 3). Comparison of the coefficient of correlation (R^2) and four error analyses (Table 5), Langmuir Type I gives the 'best fit for both MB and MV (R^2 is 0.998 and 0.995 for MB and MV, respectively). This is further confirmed by the simulated isotherm plot of calculated vs. experimental data as shown in Fig. 9 which gives a very good correlation. The q_{max} and K_L values calculated from the Langmuir Type I plot of C_e/q_e vs. C_e (Fig. 8) are 0.4949 mmol g^{-1} (158.3 mg g^{-1}) and 0.3407 mmol g^{-1} (134.2 mg g^{-1}) for MB and MV, respectively, indicating that Tarap skin is able to adsorb MB more efficiently than MV.

Webber and Chakravorti [31] defined a separation factor, R_L ,

$$R_L = \frac{1}{1 + K_L C_0}$$

which was used to describe the nature of adsorption; $R_L > 1$ being unfavorable, $0 < R_L < 1$ being favorable while $R_L = 0$ being irreversible. The adsorption isotherms for both dyes on Tarap skin were favorable with R_L values of 0.014 and 0.055 for MB and MV, respectively.

Table 4 shows the data obtained for the six different isotherm models used in this study. The isotherm constants were calculated based on the linearized form of each of these models and R^2 values, together with error functions for each isotherm model, are shown in Table 5.

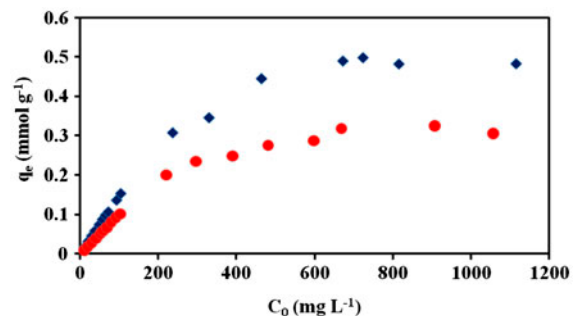


Fig. 7. Variation of the extent of removal of MB (◆) and MV (●) by Tarap skin as a function of initial dye concentration.

Table 2
Linearized forms and parameters selected for the investigation of different isotherm models

Isotherm model	Non-linear	Linear	Plot
Langmuir (Type I)	$q_e = \frac{K_L q_{max} C_e}{1 + K_L C_e}$	$\frac{C_e}{q_e} = \frac{1}{K_L q_{max}} + \frac{C_e}{q_{max}}$	$\frac{C_e}{q_e}$ vs C_e
Freundlich	$q_e = K_F C_e^{\frac{1}{n}}$	$\ln q_e = \frac{1}{n} \ln C_e + \ln K_F$	$\ln q_e$ vs $\ln C_e$
Temkin	$q_e = \frac{RT}{b} \ln K_T C_e$ where $B = \frac{RT}{b}$	$q_e = B \ln K_T + B \ln C_e$	q_e vs $\ln C_e$
D-R	$q_e = q_{max} \exp(-\beta \epsilon^2)$ $\epsilon = RT \ln[1 + \frac{1}{C_e}]$ $E = \frac{1}{\sqrt{2\beta}}$	$\ln q_e = \ln q_{max} - \beta \epsilon^2$	$\ln q_e$ vs ϵ^2
Sips	$q_e = \frac{q_{max} K_S C_e^{\frac{1}{n}}}{1 + K_S C_e^{\frac{1}{n}}}$	$\ln(\frac{q_e}{q_{max} - q_e}) = \frac{1}{n} \ln C_e + \ln K_S$	$\ln(\frac{q_e}{q_{max} - q_e})$ vs $\ln C_e$
R-P	$q_e = \frac{K_R C_e}{1 + a_R C_e^g}$	$\ln(K_R \frac{C_e}{q_e} - 1) = g \ln C_e + \ln a_R$	$\ln(K_R \frac{C_e}{q_e} - 1)$ vs $\ln C_e$

Notes: q_e is the amount of dye adsorbed, C_e is the equilibrium concentration of the dye, q_{max} is the maximum adsorption capacity, K_F ($\text{mg}^{1-1/n} \text{L}^{1/n} \text{g}^{-1}$) is the Freundlich constant, n is the empirical parameter which is related to the biosorption intensity, K_T is the equilibrium binding constant (L/mmol) corresponding to the maximum binding energy, constant B is related to the heat of adsorption, R is gas constant, and T is absolute temperature, β gives the mean free energy, E of sorption per molecule of sorbate, K_S is Sips constant, and $1/n$ is the Sips model exponent, K_R (L g^{-1}) and a_R (L mmol^{-1}) are R-P constants, and g is the exponent which lies between 0 and 1.

Table 3
Error functions

Error function	Abbreviation	Expression
Average relative error	ARE	$\frac{100}{n} \sum_{i=1}^n \left \frac{q_{e,meas} - q_{e,calc}}{q_{e,meas}} \right _i$
Sum square errors	ERRSQ	$\sum_{i=1}^n (q_{e,calc} - q_{e,meas})_i^2$
Sum of absolute error	EABS	$\sum_{i=1}^n q_{e,meas} - q_{e,calc} $
Hybrid fractional error function	HYBRID	$\frac{100}{n-p} \sum_{i=1}^n \left[\frac{(q_{e,meas} - q_{e,calc})^2}{q_{e,meas}} \right]_i$

From the simulated isotherm plots (Fig. 9) as well as from the data in Table 5, it is clear that the D-R isotherm model gave the worst fit with the lowest R^2 for MB and MV, respectively. The error analyses also showed the greatest errors, especially for MB. Further, neither the R-P model nor the Freundlich model fit the experimental data despite their reasonable R^2 values for both MB and MV.

Of all the six isotherm models used, the Langmuir, Temkin, and Sips models gave a combination of good R^2 and low errors (Tables 4 and 5). The Langmuir assumes that the adsorbate does not transmigrate in the plane of adsorbent and that there are uniform energies of adsorption on the surface.

Table 4
Parameters for adsorption of MB and MV on Tarap skin for various isotherm models

Model	Tarap skin	
	MB	MV
Langmuir		
q_{max} (mmol g^{-1})	0.4949	0.3407
K_L (L mmol^{-1})	0.0725	0.0173
R^2	0.9979	0.9949
Freundlich		
K_F (mmol g^{-1})	0.0535	0.0128
n	2.585	1.821
R^2	0.9471	0.8870
Temkin		
K_T (L mmol^{-1})	2.2079	0.2877
B	35,929	39,417
R^2	0.9648	0.9789
Dubinin-Radushkevich (D-R)		
q_{max} (mmol g^{-1})	0.2044	0.1396
β ($\text{mmol}^2 \text{J}^{-2}$)	2.0×10^{-7}	4.0×10^{-6}
R^2	0.5496	0.5702
Redlich-Peterson (R-P)		
K_R (L g^{-1})	0.099	0.05
a_R (L mmol^{-1})	0.7869	3.376
g	0.7782	0.4707
R^2	0.9907	0.8411
Sips		
q_{max} (mmol g^{-1})	0.577	0.349
K_S (L mmol^{-1})	0.0276	0.0164
n	0.6502	1.002
R^2	0.9892	0.9784

Table 5
Comparison of parameters for R^2 and error functions using different isotherm models

Dye	Model	R^2	APE	EERSQ	HYBRID	EABS
MB	Langmuir	0.9977	19.35	0.0153	0.5378	0.3532
	Freundlich	0.9471	20.36	0.0832	1.421	0.7201
	Temkin	0.9648	50.86	0.0202	0.8420	0.5012
	D–R	0.5496	4,499	121.45	14.09	15.33
	R–P	0.9907	65.56	1.2306	1.474	3.3944
	Sips	0.9892	6.92	0.0046	0.1129	0.2119
MV	Langmuir	0.9949	12.14	0.0025	0.1068	0.1795
	Freundlich	0.8870	30.71	0.0726	1.6507	0.7175
	Temkin	0.9789	36.89	0.0052	0.1744	0.2528
	D–R	0.5702	72.37	0.1827	0.2808	1.522
	R–P	0.8411	79.84	0.5823	0.2816	2.506
	Sips	0.9784	11.45	0.0027	0.1360	0.1912

Table 6
Comparison of maximum adsorption capacities of various biosorbents toward MB and MV

Adsorbent	Adsorbate	q_{\max} (mg g^{-1})	Reference
<i>A. odoratissimus</i> peel	MB	184.6	This work
Jackfruit peel	MB	285.7	[20]
Pineapple stem	MB	119.1	[34]
Coconut waste	MB	70.9	[19]
Oil palm fiber	MB	217.9	[35]
Potato leaf	MB	52.6	[32]
Tea waste	MB	85.2	[22]
Sunflower seed husk	MB	45.3	[36]
Almond shell	MB	51.0	[37]
Spent cotton seed hull	MB	185.2	[33]
<i>A. odoratissimus</i> peel	MV	137.3	This work
Orange peel	MV	11.5	[38]
Banana peel	MV	12.2	[38]
Palm kernel fibre	MV	140	[39]
Sunflower seed hull	MV	92.6	[40]
Pu-erh Tea powder (40 mesh)	MV	277.8	[41]
<i>Posidonia oceanic</i> (L.) leaf	MV	119.1	[42]
Almond shell	MV	76.3	[37]

Once adsorption takes place at the active sites of the adsorbent, it is assumed that no further adsorption occurs at that site. The Temkin isotherm model is based on the assumption that there is a linear decrease in the heat of adsorption as the adsorption progresses due to the interactions between the adsorbate and the adsorbent. The Sips isotherm model is a combination of the Langmuir and the Freundlich models, and is

Table 7
Equations for kinetic models

Kinetic models	Linear equations	Reference
Pseudo first order	$\log(q_e - q_t) = \log(q_e) - \frac{k_1}{2.303}t$	[43]
Pseudo second order	$\frac{t}{q_t} = \frac{q}{k_2 q_e^2} + \frac{1}{q_e}t$	[44]
Weber Morris intraparticle diffusion	$q_t = k_{id}t^{1/2} + C$	[45]
Elovich	$q_t = \frac{1}{\beta} \ln(\alpha\beta) + \frac{1}{\beta} \ln t$	[46]

used for heterogeneous adsorption systems. At high adsorbate concentration, the Sips model predicts a monolayer coverage, which follows the Langmuir pattern, while it approaches the Freundlich model at low adsorbate concentration.

Of these three isotherm models, error analyses show that the Sips model is the best to describe the biosorption of MB on Tarap skin. Even though the R^2 (0.9892) from the Sips model is slightly lower than that is obtained from the Langmuir model ($R^2 = 0.9979$), all the error analyses for the Sips model give much lower errors indicating that it is overall a better fit. The biosorption capacity of MB on Tarap skin is determined to be $0.577 \text{ mmol g}^{-1}$ (184.6 mg g^{-1}) based on Sips model, which is higher than the value obtained for the Langmuir model ($0.495 \text{ mmol g}^{-1}$, 158.3 mg g^{-1}).

Both the Langmuir and the Sips isotherm models gave good and compatible fitting for MV when compared to experimental data. Further, both models have reasonably close R^2 and errors between them. Hence, both models can be used to describe the adsorption isotherm of MV on Tarap skin, with the Langmuir model giving a better R^2 and lower errors in general. These results indicate that adsorption of MB on Tarap skin is stronger than that of MV on the same adsorbent. This could be due to the less bulky nature of MB than that of MV, enabling more MB molecules to be adsorbed on the Tarap skin.

Table 6 shows the biosorption capacity of MB and MV, obtained from the Sips isotherm, in comparison with the results of some reported low-cost biosorbents, based on the best experimental condition of each work. Although Tarap skin has lower biosorption capacity for MB as compared to some biosorbents, such as jackfruit peel and oil palm, it can be considered as a good biosorbent as it is able to remove MB better than many other biosorbents, such as tea waste [22], coconut waste [19], and potato leaf [32]. Its biosorption capacity is only slightly lower than spent

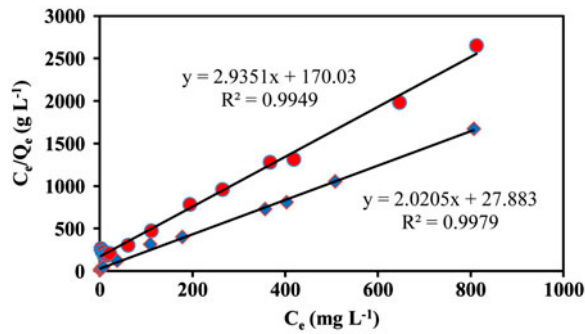


Fig. 8. Linear Langmuir Type I plot for sorption of MB (♦) and MV (●) on Tarap skin.

cotton seed hull [33]. On the other hand, Tarap skin has a great potential as a strong biosorbent for MV as it gives higher q_{max} value than that of many reported low-cost biosorbents given in the table. Apart from oven drying, Tarap skin used in this study was not chemically treated. Hence, there is a possibility that its adsorption capacity could be further enhanced through chemical modification.

3.5. Kinetics of biosorption of MB and MV on Tarap skin

The sorption mechanism of MB and MV on Tarap skin was further elaborated using the pseudo first

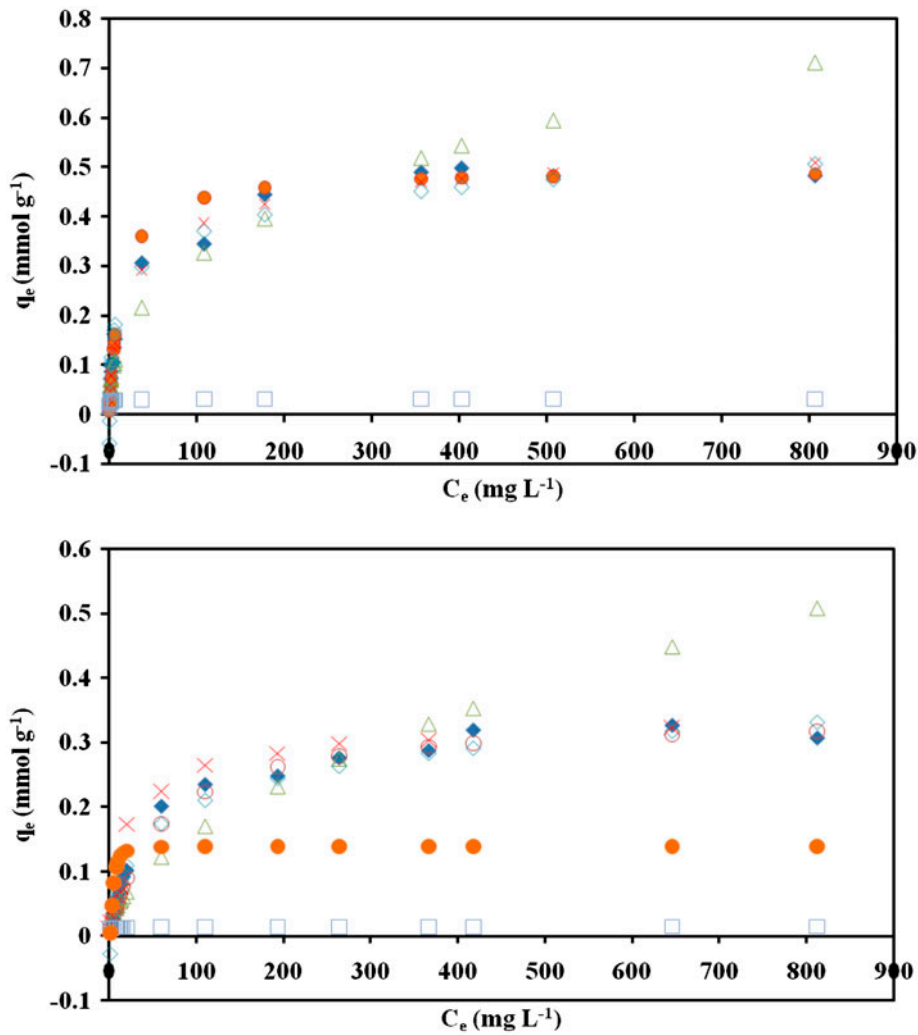


Fig. 9. Different isotherm models for adsorption of MB (top) and MV (bottom) on Tarap skin (♦) Experimental, (o) Langmuir, (Δ) Freundlich, (×) Sips, (◇) Temkin, (□) R-P, and (●) D-R.

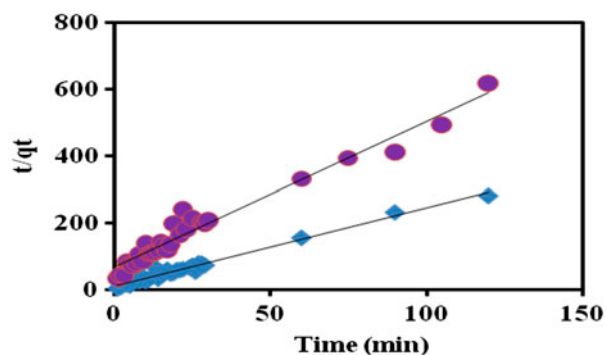


Fig. 10. Pseudo-second-order kinetics model for adsorption of MB (♦) and MV (•) on Tarap skin.

order [43], pseudo-second-order [44], the Weber Morris intraparticle diffusion [45] and Elovich [46] models. Equations of kinetics models are listed in Table 7 where q_e and q_t (mmol g^{-1}) are the amount of dye adsorbed at equilibrium and at time t (min), k_1 (min^{-1}) is the pseudo-first-order rate constant; k_2 ($\text{g mmol}^{-1} \text{min}^{-1}$) is the pseudo-second-order rate constant; k_{id} ($\text{mmol g}^{-1} \text{min}^{-1}$) is intraparticle diffusion rate constant; C is a measure of the thickness of boundary layer; α ($\text{mmol g}^{-1} \text{min}^{-1}$) is the initial sorption rate and β (mmol g^{-1}) is related to the extent of surface coverage and activation energy for chemisorption. The kinetics was very rapid for the biosorption of 10.0 mg L^{-1} dye on Tarap skin with more than 50%

dye being adsorbed within the first minute. Such fast kinetics provides highly favorable conditions for the bioremediation of wastewater contaminated with MB and MV.

However, under such rapid adsorption, pseudo-kinetic models cannot be applied for low concentrations, as pseudo models require the concentration of a reactant to be in large excess. Hence, dye solutions of high concentrations ($1,000 \text{ mg L}^{-1}$ MB and 500 mg L^{-1} MV) were chosen, whereby the extent of removal of each dye was kept below 30%, satisfying the pseudo-order condition.

From Fig. 10, it can be seen that kinetics for the biosorption of both MB and MV on Tarap skin follows the pseudo-second-order model with R^2 0.9809 and 0.9617 for MB and MV, respectively. The rate constants obtained from the above model are 0.5373 and $0.2859 \text{ g mmol}^{-1} \text{ min}^{-1}$, for MB and MV, respectively. The R^2 values obtained for other three kinetics models are less than 0.9, and the majority of the data do not fall on a straight line, indicating that these models are inappropriate. This is especially true for MB where all R^2 was found to be below 0.5.

3.6. FTIR spectroscopic investigation of Tarap skin

It can be seen from FTIR (Fig. 11) spectra that, upon treatment of Tarap skin with dye, the wavelength of the broadband at $3,319 \text{ cm}^{-1}$ is decreased to

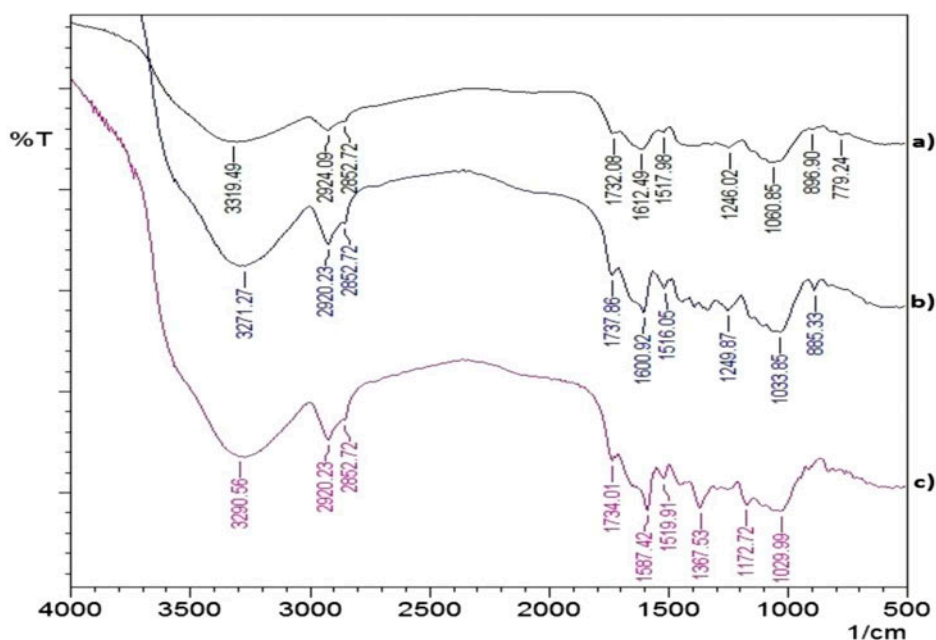


Fig. 11. FTIR spectra of Tarap skin (a) untreated (b) after adsorption with MB, and (c) after adsorption with MV.

3,271 and 3,290 cm^{-1} for MB and MV, respectively, indicating that hydroxyl and amino groups are involved in bond formation with dyes. A prominent decrease in wavelength is observed for C=O stretching of the carboxylic acid peak from 1,612 to 1,601 cm^{-1} and 1,587 cm^{-1} for both MB and MV, respectively, indicating that carboxylic acid groups play a significant role in the adsorption of both dyes.

4. Conclusion

The peel of *A. odoratissimus* can be successfully utilized as a low-cost biosorbent for the removal of cationic dyes, namely MB and MV. The adsorption isotherm for MB fits the Sips isotherm model, while that for MV corresponds to both the Langmuir and Sips models with regression coefficients close to 1 and very low error functions as compared to other isotherm models. It is thus proposed that the dyes are preferentially adsorbed as a monolayer at low concentrations with their flat orientation, and hence, incorporation of dye molecules to the bulk of the adsorbent is unlikely in contrast to the sorption of metal ions. The adsorption capacity for MB (184.6 mg g^{-1}) is comparable to many reported biosorbents while that for MV (137.3 mg g^{-1}) is superior to many low-cost biosorbents reported. Thus, *A. odoratissimus* skin is proven to be a potential low-cost biosorbent for the removal of these dyes. Kinetics of adsorption of both dyes was fast and followed the pseudo-second-order. The adsorption capacity could possibly be further enhanced by chemical modification.

Acknowledgments

The authors thank the Government of Brunei Darussalam and the Universiti Brunei Darussalam (UBD) for their financial support. The authors are also grateful to the Energy Research Group and the Department of Biology at UBD for the use of XRF and SEM, respectively.

References

- [1] R. Singh, Production of high-purity water by membrane processes, *Desalin. Water Treat.* 3 (2009) 99–110.
- [2] S.I. Abou-Elela, M.A. El-Khateeb, Treatment of ink wastewater via heterogeneous photocatalytic oxidation, *Desalin. Water Treat.* 7 (2009) 1–5.
- [3] K. Turhan, Z. Turgut, Treatment and degradability of direct dyes in textile wastewater by ozonation: A laboratory investigation, *Desalin. Water Treat.* 11 (2009) 184–191.
- [4] N. Zaghbani, A. Hafiane, M. Dhahbi, Removal of direct blue 71 from wastewater using micellar enhanced ultrafiltration, *Desalin. Water Treat.* 6 (2009) 204–210.
- [5] P. Sharma, H. Kaur, M. Sharma, V. Sahore, A review on applicability of naturally available adsorbents for the removal of hazardous dyes from aqueous waste, *Environ. Monit. Assess.* 183 (2011) 151–195.
- [6] M.S.U. Rehman, I. Kim, J.-I. Han, Adsorption of methylene blue dye from aqueous solution by sugar extracted spent rice biomass, *Carbohydr. Polym.* 90 (2012) 1314–1322.
- [7] D. Sud, G. Mahajan, M.P. Kaur, Agricultural waste material as potential adsorbent for sequestering heavy metal ions from aqueous solutions—A review, *Bioresour. Technol.* 99 (2008) 6017–6027.
- [8] T. Sulak, H.C. Yatmaz, Removal of textile dyes from aqueous solutions with eco-friendly biosorbent, *Desalin. Water Treat.* 37 (2012) 169–177.
- [9] G. Crini, Non-conventional low-cost adsorbents for dye removal: A review, *Bioresour. Technol.* 97 (2006) 1061–1085.
- [10] L.B.L. Lim, N. Priyantha, D.T.B. Tennakoon, H.I. Chieng, C. Bandara, Sorption characteristics of peat of Brunei Darussalam I: Characterization of peat and adsorption equilibrium studies of methylene blue—Peat interactions, *Cey. J. Sci.* 17 (in press).
- [11] N. Priyantha, L.B.L. Lim, M.K. Dahri, D.T.B. Tennakoon, Dragon fruit skin as potential low-cost biosorbent for the removal of manganese(II) ions, *J. Appl. Sci. Environ. Sanit.* 8 (2013) 179–188.
- [12] A. Demirbas, Agricultural based activated carbons for the removal of dyes from aqueous solutions: A review, *J. Hazard. Mater.* 167 (2009) 1–9.
- [13] P.L. Tan, C.L. Wong, S.L. Hii, Investigation on adsorptive removal of basic dye by seaweed-derived biosorbent: Considering effects of sorbent dosage, ionic strength and agitation speed, *Desalin. Water Treat.* 48 (2012) 238–244.
- [14] Y.P. Tang, B.L.L. Linda, L.W. Franz, Proximate analysis of *Artocarpus odoratissimus* (Tarap) in Brunei Darussalam, *Int. Food Res. J.* 20 (2013) 409–415.
- [15] L.B.L. Lim, N. Priyantha, D.T.B. Tennakoon, M.K. Dahri, Biosorption of cadmium(II) and copper(II) ions from aqueous solution by core of *Artocarpus odoratissimus*, *Environ. Sci. Pollut. Res.* 19 (2012) 3250–3256.
- [16] N. Priyantha, L.B.L. Lim, D.T.B. Tennakoon, N.H.M. Mansor, M.K. Dahri, H.I. Chieng, Breadfruit (*Artocarpus altilis*) waste for bioremediation of Cu(II) and Cd(II) ions from aqueous medium, *Cey. J. Sci.*, 17 (in press).
- [17] M.R. Malekbala, S. Hosseini, S. Kazemi Yazdi, S. Masoudi Soltani, M.R. Malekbala, The study of the potential capability of sugar beet pulp on the removal efficiency of two cationic dyes, *Chem. Eng. Res. Des.* 90 (2012) 704–712.
- [18] L.S. Balistrieri, J.W. Murray, The surface chemistry of goethite (α -FeOOH) in major ion seawater, *Amer. J. Sci.* 281 (1981) 788–806.
- [19] B.H. Hameed, D.K. Mahmoud, A.L. Ahmad, Equilibrium modeling and kinetic studies on the adsorption of basic dye by a low-cost adsorbent: Coconut (*Cocos nucifera*) bunch waste, *J. Hazard. Mater.* 158 (2008) 65–72.

- [20] B.H. Hameed, Removal of cationic dye from aqueous solution using jackfruit peel as non-conventional low-cost adsorbent, *J. Hazard. Mater.* 162 (2009) 344–350.
- [21] B.H. Hameed, D.K. Mahmoud, A.L. Ahmad, Sorption of basic dye from aqueous solution by pomelo (*Citrus grandis*) peel in a batch system, *Colloids Surf., A* 316 (2008) 78–84.
- [22] M.T. Uddin, M.A. Islam, S. Mahmud, M. Rakanuzzaman, Adsorptive removal of methylene blue by tea waste, *J. Hazard. Mater.* 164 (2009) 53–60.
- [23] M.T. Uddin, M. Rakanuzzaman, M.M.R. Khan, M.A. Islam, Adsorption of methylene blue from aqueous solution by jackfruit (*Artocarpus heterophyllus*) leaf powder: A fixed-bed column study, *J. Environ. Manage.* 90 (2009) 3443–3450.
- [24] C.H. Giles, T.H. MacEwan, S.N. Nakhwa, D. Smith, Studies in adsorption. Part XI. A system of classification of solution adsorption isotherms, and its use in diagnosis of adsorption mechanisms and in measurement of specific surface areas of solids, *J. Chem. Soc.* (1960) 3973–3993.
- [25] I. Langmuir, The constitution and fundamental properties of solids and liquids. Part I. Solids, *J. Amer. Chem. Soc.* 38 (1916) 2221–2295.
- [26] H.M.F. Freundlich, Über die adsorption in losungen (Adsorption in solution), *Z. Phys. Chem.* 57 (1906) 384–470.
- [27] M.I. Temkin, V. Pyzhev, Kinetics of ammonia synthesis on promoted iron catalyst, *Acta. Physichem. USSR.* 12 (1940) 327–356.
- [28] M.M. Dubinin, L.V. Radushkevich, The equation of the characteristic curve of the activated charcoal. *Proc. Acad. Sci. USSR Phys. Chem. Sec.* 55 (1947) 331–337.
- [29] O. Redlich, D.L. Peterson, A useful adsorption isotherm, *J. Phys. Chem.* 63 (1959) 1024.
- [30] R. Sips, Combined form of Langmuir and Freundlich equations, *J. Chem. Phys.* 16 (1948) 490–495.
- [31] W.J. Weber, J.C. Morris, Pore and solid diffusion models for fixed bed adsorbers, *AIChE J.* 20 (1974) 228–238.
- [32] N. Gupta, A.K. Kushwaha, M.C. Chattopadhyaya, Application of potato (*Solanum tuberosum*) plant wastes for the removal of methylene blue and malachite green dye from aqueous solution, *Arab. J. Chem.* <http://dx.doi.org/10.1016/j.arabjc.2011.07.021>.
- [33] Q. Zhou, W. Gong, C. Xie, X. Yuan, Y. Li, C. Bai, S. Chen, N. Xu, Biosorption of methylene blue from aqueous solution on spent cottonseed hull substrate for *Pleurotus ostreatus* cultivation, *Desalin. Water Treat.* 29 (2011) 317–325.
- [34] B.H. Hameed, R.R. Krishni, S.A. Sata, A novel agricultural waste adsorbent for the removal of cationic dye from aqueous solutions, *J. Hazard. Mater.* 162 (2009) 305–311.
- [35] A.E. Ofomaja, Sorption dynamics and isotherm studies of methylene blue uptake on to palm kernel fibre, *Chem. Eng. J.* 126 (2007) 35–43.
- [36] S. Ong, P. Keng, S. Lee, M. Leong, Y. Hung, Equilibrium studies for the removal of basic dye by sunflower seed husk (*Helianthus annuus*), *Int. J. Phys. Sci.* 5 (2010) 1270–1276.
- [37] C. Duran, D. Ozdes, A. Gundogdu, H.B. Senturk, Kinetics and isotherm analysis of basic dyes adsorption onto almond shell (*Prunus dulcis*) as a low cost adsorbent, *J. Chem. Eng. Data* 56 (2011) 2136–2147.
- [38] G. Annadurai, R.S. Juang, D.J. Lee, Use of cellulose-based wastes for adsorption of dyes from aqueous solutions, *J. Hazard. Mater.* 92 (2002) 263–274.
- [39] A.E. Ofomaja, E.E. Ukpebor, S.A. Uzoekwe, Biosorption of methyl violet onto palm kernel fiber: Diffusion studies and multistage process design to minimize biosorbent mass and contact time, *Biomass Bioenergy* 35 (2011) 4112–4123.
- [40] B.H. Hameed, Equilibrium and kinetic studies of methyl violet sorption by agricultural waste, *J. Hazard. Mater.* 154 (2008) 204–212.
- [41] P. Li, Y.J. Su, Y. Wang, B. Liu, L.M. Sun, Bioadsorption of methyl violet from aqueous solution onto Pu-erh tea powder, *J. Hazard. Mater.* 179 (2010) 43–48.
- [42] S. Cengiz, L. Cavas, A promising evaluation method for dead leaves of *Posidonia oceanica* (L.) in the adsorption of methyl violet, *Marine Biotechnol.* 6 (2010) 728–736.
- [43] S. Lagergren, Zur theorie der sogenannten adsorption gelöster stoffe [About the theory of so-called adsorption of soluble substances], *KungligaSvenska. Vetenskapsakademiens. Handlingar.* 28 (1898) 1–39.
- [44] Y.S. Ho, G. McKay, Sorption of dye from aqueous solution by peat, *Chem. Eng. J.* 70 (1998) 115–124.
- [45] W.J. Weber, J.C. Morris, Kinetics of adsorption on carbon from solution, *J. Sanit. Eng. Div.* 89 (1963) 31–60.
- [46] R.S. Juang, M.L. Chen, Application of the Elovich equation to the kinetics of metal sorption with solvent-impregnated resins, *Ind. Eng. Chem. Res.* 36 (1997) 813–820.